



Correlative Surface Imaging Reveals Chemical Signatures for Bacterial Hotspots on Plant Roots

Journal:	<i>Analyst</i>
Manuscript ID	AN-ART-10-2019-001954.R1
Article Type:	Paper
Date Submitted by the Author:	31-Oct-2019
Complete List of Authors:	<p>Liu, Wen; Pacific Northwest National laboratory, Environmental Molecular Sciences Laboratory; China University of Geosciences, BGEG Huang, Liuqin; State Key Laboratory of Biogeology and Environmental Geology, China University of Geosciences, Wuhan 430074, China; Pacific Northwest National laboratory, Environmental Molecular Sciences Laboratory Komorek, Rachel; Pacific Northwest National Laboratory , Atmospheric Sciences and Global Change Division Handakumbura, Pubudupinipa; Pacific Northwest National laboratory, Environmental Molecular Sciences Laboratory Zhou, Yadong; Pacific Northwest National laboratory, Environmental Molecular Sciences Laboratory Hu, Dehong; Pacific Northwest National laboratory, Environmental Molecular Sciences Laboratory Engelhard, Mark; Pacific Northwest National laboratory, Environmental Molecular Sciences Laboratory Jiang, Hongchen ; China University of Geosciences, BGEG Yu, Xiao-Ying; Pacific Northwest National Laboratory , Atmospheric Sciences and Global Change Division Jansson, Christer; Pacific Northwest National laboratory, Environmental Molecular Sciences Laboratory Zhu, Zihua; Pacific Northwest National Laboratory , Environmental Molecular Sciences Laboratory</p>

1
2
3 **Correlative Surface Imaging Reveals Chemical Signatures for Bacterial**
4 **Hotspots on Plant Roots**
5
6
7

8 Wen Liu^{1,2#}, Liuqin Huang^{1,2#}, Rachel Komorek³, Pubudu P. Handakumbura¹, Yadong Zhou¹, Dehong
9 Hu¹, Mark H Engelhard¹, Hongchen Jiang², Xiao-Ying Yu³, Christer Jansson¹, Zihua Zhu^{1*}
10

11 ¹ Environmental Molecular Science Laboratory, Pacific Northwest National Laboratory, Richland, WA
12 99354, USA

13 ² State Key Laboratory of Biogeology and Environmental Geology, China University of Geosciences,
14 Wuhan, 430074, China

15 ³ Earth and Biological Sciences Directorate, Pacific Northwest National Laboratory, Richland, WA
16 99354, USA
17

18 Email: Zihua.zhu@pnnl.gov

19 #: Equal contribution
20
21
22
23
24
25
26
27
28
29
30
31
32
33
34
35
36
37
38
39
40
41
42
43
44
45
46
47
48
49
50
51
52
53
54
55
56
57
58
59
60

Abstract

The rhizosphere is arguably the most complex microbial habitat on earth, comprising an integrated network of plant roots, soil and a highly diverse microbial community (the rhizosphere microbiome)¹. Understanding, predicting and controlling plant-microbe interactions in the rhizosphere will allow us to harness the plant microbiome as a means to increase or restore plant ecosystem productivity, improve plant responses to a wide range of environmental perturbations, and mitigate effects of climate change by designing ecosystems for long-term soil carbon storage¹. To this end, it is imperative to develop new molecular approaches with high spatial resolution to capture interactions at the plant-microbe, microbe-microbe, and plant-plant interfaces. In this work, we designed an imaging sample holder that allows integrated surface imaging tools to map the same locations of a plant root-microbe interface with submicron lateral resolutions, providing novel *in vivo* analysis of root-microbe interactions. Specifically, confocal fluorescence microscopy, time-of-flight secondary ion mass spectrometry (ToF-SIMS), X-ray photoelectron spectroscopy (XPS), and scanning electron microscope (SEM) were used for the first time for correlative imaging of the *Brachypodium distachyon* root and its interaction with *Pseudomonas* SW25, a typical plant growth-promoting soil bacterium. Imaging data suggest that the root surface is inhomogeneous and that the interaction between *Pseudomonas* and *Brachypodium* roots was confined to only few spots along the sampled root segments and that the bacterial attachment spots were enriched in Na- and S-related and high-mass organic species. We conclude that attachment of the *Pseudomonas* cells to the root surface is outcompeted by strong root-soil mineral interactions but facilitated by formation of extracellular polymeric substances (EPS).

Key words.

Plant root, Plant growth-promoting bacteria, Soil, Correlative surface imaging, ToF-SIMS, Fluorescence microscopy, SEM

Introduction

The rhizosphere, i.e., the thin region surrounding and including roots, is a well-known hotspot for microbial activity and abundance (the rhizosphere microbiome) due to the enrichment of root exudates and debris.² Some members of the rhizosphere microbiome, referred to as plant growth-promoting bacteria (PGPB)^{3, 4} can stimulate plant growth and productivity by reducing pathogenic infection⁵, enhancing tolerance to abiotic stress such as drought⁶, or increasing the provision of nutrients like P and N^{7, 8}. Application of PGPB has proved to be promising as bio-fertilizers or pesticides, which can significantly reduce environmental pollution from the overuse of chemical fertilizers (e.g., N, P) and toxic pesticides in cropping systems.^{9, 10} However, rhizosphere interactions are a complex function of biotic and abiotic factors, making it difficult to translate findings from PGPB inoculations performed under controlled laboratory conditions to the stochastic field environment.^{11, 12} Thus, detailed, molecular and elemental understanding of plant-microbe interactions in the rhizosphere is vital for our ability to fully harness the rhizosphere microbiome for agricultural applications.¹³

Brachypodium distachyon (Brachypodium) is a widely distributed annual monocot grass that has been proposed as a model organism for grasses, including bioenergy grasses due to its suitable traits such as small genome, short lifetime, simple growth conditions and amenability to genetic modification.^{14, 15, 16, 17} It has been widely used for many fundamental studies including plant-microbe interactions^{18, 19, 20, 21}. *Pseudomonas* sp. are commonly found in the rhizosphere and many isolates (e.g., *Pseudomonas* SW25 used in this study²² and *P. fluorescens*²³) have been widely studied as model PGPB. However, the mechanisms of *Pseudomonas* on promoting plant growth are still under debate and may include pathogen suppression, P release, N fixation and hormonal regulation.²³⁻²⁵ Even less is known about the fundamental principles that control the interactions between plant roots and the *Pseudomonas* bacteria.

The rhizosphere is a highly heterogeneous system, mainly composed of roots, mineral particles, organic matters and various microbes¹. Most commonly used analysis tools in this field such as total carbon analysis,²⁶ FT-ICR-MS, NMR,²⁷ and genomics²⁸ are bulk analysis techniques, i.e., samples need to be extracted from the system using solvents. Although such approaches have provided key information for developing various models to explain mass transfer in the rhizosphere, they are associated with at least two intrinsic drawbacks. First, these approaches lack spatial information to describe the distribution of microbes or organic matter, e.g., along a root segment. Second, although some organic or bioorganic molecules are soluble, many molecular species may not be soluble, and/or be firmly attached to mineral or root surfaces. Scanning electron microscopy (SEM)²⁹ and transmission electron microscopy (TEM)³⁰ have been introduced in the field, providing morphological information with good spatial resolution, albeit with mostly elemental and no or little molecular information. Traditionally, fluorescence microscopy has been widely used in this field, and recently nanoscale secondary ion mass spectrometry (NanoSIMS) has been employed to map the distribution of organic matter on mineral surfaces³¹. These techniques can provide high spatial-resolution (down to tens of a nm) chemical maps, although, generally, only select species with specially labelled fluorescent or isotope tags can be tracked.

Time-of-flight secondary ion mass spectrometry (ToF-SIMS) is a powerful surface analysis tool with several unique advantages.³² First, it can provide elemental, isotopic and molecular information simultaneously. Second, its information depth is very shallow (normally 1-3 nm), so surface-specific information can be collected. In addition, it has excellent sensitivity

(ppm level) and very good spatial resolution (sub-micron)³³. Therefore, it is a very useful tool in studies of rhizosphere. Clearly, each technique has its own strength and weaknesses, and a single technique normally can provide only limited information. Therefore, a multi-technique approach is highly desirable for comprehensive interrogation of a complex system such as the rhizosphere.

In this work, confocal fluorescence microscopy, ToF-SIMS, X-ray photoelectron spectroscopy (XPS) and SEM were collectively used for the first time to image the *Brachypodium* root and root-microbe interactions.

Materials and Methods

Four *Brachypodium* plants (named U1, U3, I1, I2) were grown. The U1 and U3 plants were used as reference (without *Pseudomonas* treatment), and the I1 and I2 plants were treated with *Pseudomonas*. In brief, *Brachypodium distachyon*, reference line Bd21 was used as the plant system. Soil from PNNL's field site in Prosser, WA, United States was used as the growing medium. The Prosser soil is characterized as a Warden fine sandy/silt loam with 0.4% organic matter and 1 mg/kg ammonium N per dry weight. *Brachypodium* seeds were sown on sterilized (autoclaved) Prosser soil and placed in a Percival growth chamber with 16:8 h light:dark cycles with 22:18 °C day: night temperatures, 60 % RH, and ~250 $\mu\text{moles m}^{-2} \text{s}^{-1}$ light intensity. *Pseudomonas fluorescens SW25* bacteria, which expressed green fluorescence protein (GFP), were injected into the soil surrounding the I1 and I2 plants at 3 weeks post germination; the bacteria were grown to log phase OD600, pelleted and re-suspend to a specific OD = 0.6-0.8 before pipetting them into the soil/base of each plant. At the end of the experiment root samples were harvested for subsequent analysis.

Two root segments (about 12-15 mm each) close to the bacterial inoculation areas were selected and excised from each of the I1 and I2 plants. Similarly, two roots from the corresponding areas were selected and cut from each of the U1 and U3 plants. The roots were gently rinsed with deionized water to remove loosely attached soil particles, and then immobilized onto a special sample holder (**Fig. 1a**) that was developed as part of this study. In brief, eight stainless steel pins were used to immobilize four molybdenum (Mo) masks on a ~5.0 cm diameter aluminum (Al) sample holder (thickness ~6.0 mm). Four Mo masks (12.7 mm diameter and 0.10 mm thick each) were used to press root samples to make them flat. Sample flatness was critical to ensure high quality data from surface analysis tools such as ToF-SIMS and XPS. On each Mo mask, three 5.0 \times 1.5 mm² windows were open for imaging analysis. Such a design allowed us to easily determine accurate locations for multi-imaging analysis. For example, as shown in Figure 1b, two root samples were immobilized under a Mo mask, and six selected locations, including locations (1) and (2), could be easily located and imaged using different imaging tools.

Initial analysis of fresh root segments was performed by fluorescence microscopy using an upright confocal fluorescence microscope (Zeiss LSM 710) under ambient condition. The excitation is Ar ion laser with a 488 nm wavelength. The objective is 40X NA 0.75. The fluorescence detection has wavelength range of 498 nm to 550 nm for GFP. 3D Z stack was acquired for every sample. The locations of fluorescence images were recorded for subsequent ToF-SIMS, XPS and SEM imaging analysis.

1
2
3 Fluorescence microscopy was followed by ToF-SIMS imaging using a TOF-SIMS5 instrument
4 (IONTOF GmbH, Münster, Germany). Before SIMS analysis, the sample holder was put into the
5 introduction chamber of the SIMS instrument, and the root samples were dried under vacuum.
6 After drying, the sample holder was introduced into the analysis chamber for SIMS imaging
7 analysis. A 25 keV Bi_3^+ beam was used as the analysis beam to collect SIMS spectra and images.
8 The Bi_3^+ beam was focused to be $\sim 0.5 \mu\text{m}$ diameter and scanned over $200 \times 200 \mu\text{m}^2$ to 500×500
9 μm^2 areas. The current of the Bi_3^+ beam was about 0.36 pA with 10 kHz pulse frequency, and data
10 collection time was 600 s per imaging testing. The total ion dose was under the static limit so only
11 surface information ($< 2 \text{ nm}$) was collected. While collecting data, a low energy electron flood gun
12 (10 eV, $\sim 1.0 \mu\text{A}$ current) was used to compensate for surface charging. The pressure in the analysis
13 chamber was about 2×10^{-8} mbar. A positive ion imaging testing and a negative ion imaging testing
14 were performed on each selected location (totally 24 locations, 6 on each Mo mask, as shown in
15 Figure 1a and 1b). Due to the complexity of ToF-SIMS spectral data, principle component analysis
16 (PCA)^{34, 35} was used to extract effective information, following procedures described in our
17 previous work³⁶⁻³⁸. Because only SIMS signals on root surface are of interest for PCA analysis,
18 data reconstruction was required. SIMS imaging capability shows its importance here. During data
19 reconstruction, only root surface areas were selected based on SIMS images (e.g., **Fig. 1d**). Thus,
20 SIMS signals on root surfaces were shown in reconstructed mass spectra for further PCA analysis,
21 and interference signals from substrate could be removed.
22
23
24
25

26 XPS measurements were conducted on the same samples after ToF-SIMS analysis. A Physical
27 Electronics Quantera Scanning X-ray Microprobe was used. This system uses a focused
28 monochromatic Al $\text{K}\alpha$ X-ray (1486.7 eV) source for excitation and a spherical section analyzer.
29 The instrument has a 32-element multichannel detection system. The X-ray beam is incident
30 normal to the sample and the photoelectron detector is at 45° off-normal. High energy resolution
31 spectra were collected on root surfaces using a pass-energy of 69.0 eV with a step size of 0.125
32 eV. For the Ag $3d_{5/2}$ line, these conditions produced a FWHM of $0.92 \text{ eV} \pm 0.05 \text{ eV}$. The binding
33 energy (BE) scale is calibrated using the Cu $2p_{3/2}$ feature at $932.62 \pm 0.05 \text{ eV}$ and Au $4f_{7/2}$ at 83.96
34 $\pm 0.05 \text{ eV}$. The sample experienced variable degrees of charging. Low energy electrons at $\sim 1 \text{ eV}$,
35 $19 \mu\text{A}$ and low energy Ar^+ ions were used to minimize this charging.
36
37

38 SEM imaging was performed after the XPS measurements. A Hitachi TM-1000 scanning electron
39 microscope (Chiyoda, Tokyo, Japan) was used with an accelerating voltage of 15.0 kV. Before
40 SEM imaging, about 2 nm Au was coated on top of the sample to reduce charging. The imaging
41 areas were ranging from $100 \times 75 \mu\text{m}^2$ to $500 \times 375 \mu\text{m}^2$.
42

43 **Results and Discussions**

44

45 Fluorescence was used to assess whether or not *Pseudomonas* cells were evenly distributed on the
46 Brachypodium root surface. Interestingly, we found that attachment of *Pseudomonas* was obvious
47 at only two locations on the root, locations (1) and (2) of the I2 plant (**Fig. 1b**).
48
49
50
51
52
53
54
55
56
57

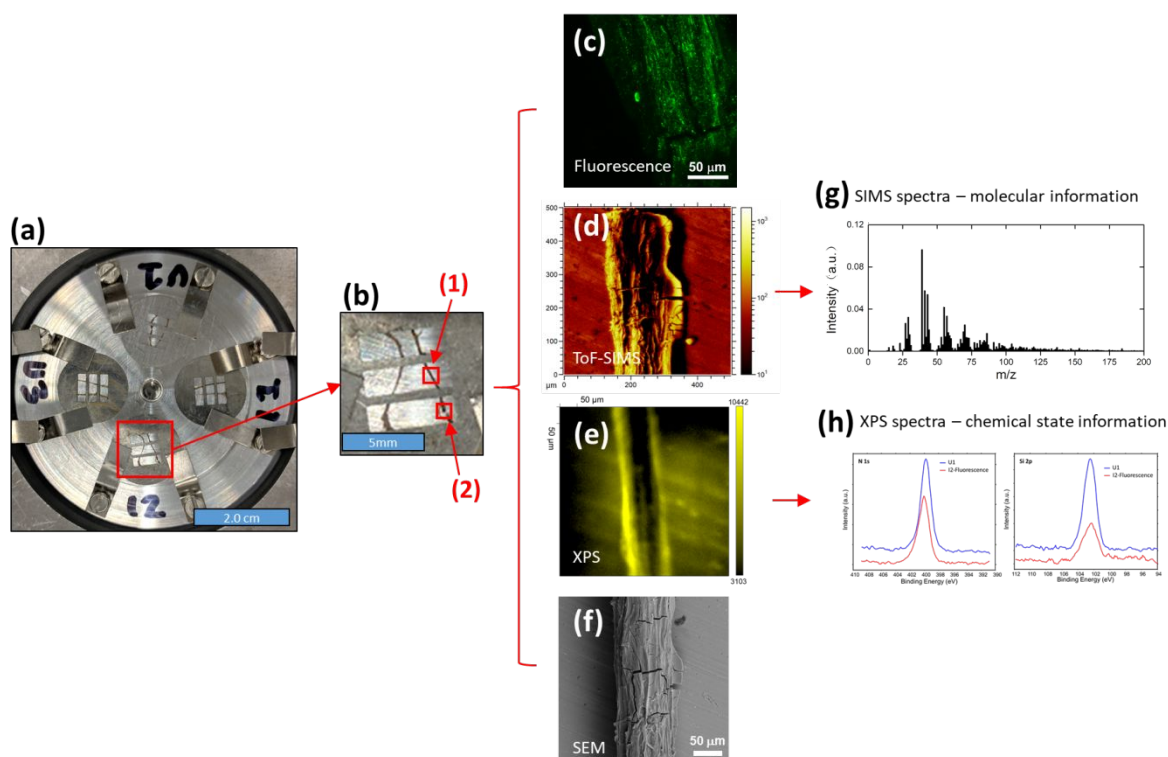


Figure 1. Development of a universal sample holder for correlative imaging analysis of plant root samples using a multi-pronged surface analysis approach. (a) The Al sample holder with eight *Brachypodium* root samples. The U1 and U3 samples were cut from two *Brachypodium* plants without *Pseudomonas* inoculation. The I1 and I2 samples were cut from two *Brachypodium* plants after *Pseudomonas* inoculation. Two root segments were selected and excised from each plant. (b) A zooming-in of the I2 samples. A Mo mask was used to immobilize root segments. Imaging analysis was performed through three $5.0 \times 1.5 \text{ mm}^2$ windows. Six locations, e.g., locations (1) and (2) in (b), could be imaged by fluorescence (c), ToF-SIMS (d), XPS (e) and SEM (f). SIMS and XPS spectra ((g) and (h)) were collected for chemical information. The initial imaging by fluorescence microscopy indicated that *Pseudomonas* attached on the roots only at locations (1) and (2).

The fluorescence microscopy results prompted the question of how the surface properties of the attachments spots differed from the rest of the root. Here, ToF-SIMS spectra (**Fig. 2**) can provide valuable chemical information, including elemental, isotopic and molecular information, to elucidate the difference. However, ToF-SIMS spectra are complex, and each spectrum may be composed of hundreds of ion signals. Thus, statistical analysis was used to distinguish features that differentiate the regions with and without *Pseudomonas*.

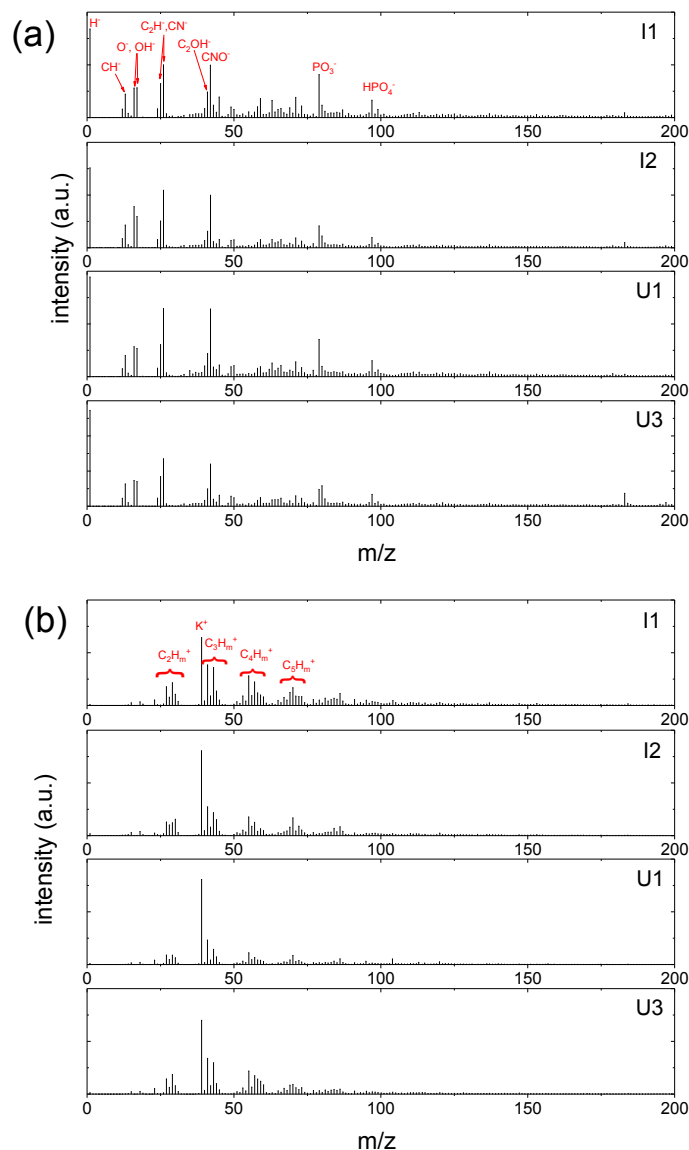


Figure 2. Representative ToF-SIMS spectra of I1, I2, U1 and U3 samples. (a) negative ion spectra; (b) positive ion spectra.

Principle Component Analysis (PCA) has been widely used in ToF-SIMS data analysis for over a decade. Figure 3 shows PCA analysis results of negative ion spectra collected from four set of *Brachypodium* root samples. The PC1 scores plot (**Fig. 3a**) revealed that only two spots were clearly separated. It should be noted that after PCA analysis, each spectrum has its own PC1 score value; that is to say, each data spot in Figure 3a is corresponding to a spectrum. Thus, based on the PC1 score values, these two separated data spots are found to be corresponding to the spectra from the locations (1) and (2) of the I2 sample (**Fig. 1b**). The two separated data spots are close to each other, and the major difference between them and the remaining data spots is the decrease in PC1 scores. The PC1 loadings plot (**Fig. 3b**) shows that the positive loadings of PC1 are mainly CN and PO_x -related species, as well as low-mass organic species, while the negative PC1 loadings are mainly Cl and organic SO_x species, as well as high-mass organic species. The loadings plot data

suggest that the surface of attachment spots for the *Pseudomonas* cells had relatively more Cl, organic SO_x and high-mass organic species, but less CN, PO_x-related species and low-mass organic species. Moreover, the PC1 scores of the remaining data spots are close together, suggesting that all *Pseudomonas*-free root surfaces exhibited similar micro-chemical environment.

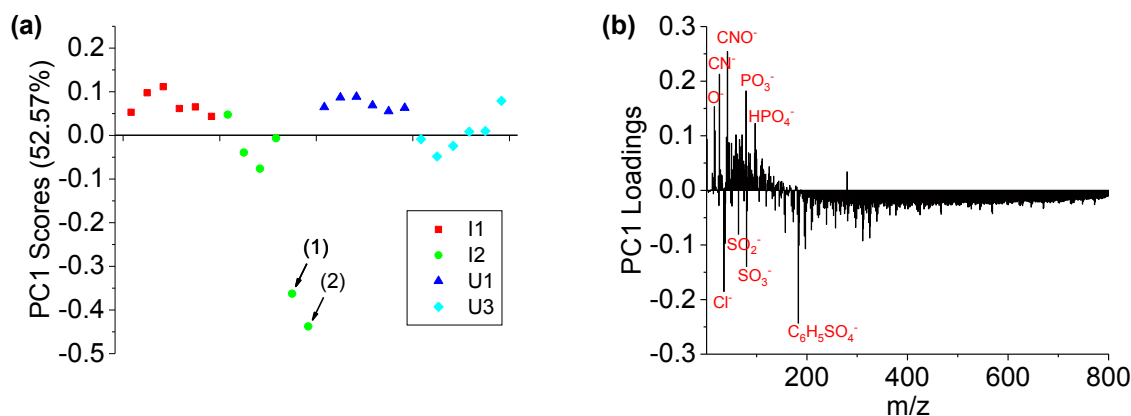


Figure 3. PCA analysis results of negative ion spectra of I1, I2, U1 and U3 samples (Fig. 2). (a) PC1 scores plot; (b) PC1 loadings plot. It should be noted that the data spots (1) and (2) in (a) correspond to the two locations (1) and (2) in Fig. 1b, where *Pseudomonas* attachment was observed.

Figure 4 shows PCA analysis results of positive ion spectra collected from the four sets of *Brachypodium* root samples. The PCA scores plot (**Fig. 4a**) is qualitatively consistent with the negative ion results. The PC1 scores of locations (1) and (2) are well separated from the remaining data spots. The loadings plot (**Fig. 4b**) shows that the major positive loadings of PC1 are Na-related species and high-mass organic species, and the negative loadings are K⁺, NH₄⁺ and low-mass organic N species. The data suggest that the root surface of the *Pseudomonas* attachment spots had relatively more Na-related species and high-mass organic species, but less K⁺, NH₄⁺ and low-mass organic N species.

Importantly, PCA analysis results from negative ion spectra and positive ion spectra are consistent with each other. First, PC1 scores could separate *Pseudomonas* attachment spots from *Pseudomonas*-free root segments. Second, both positive ion results and negative ion results show that small N-contained organic species are enriched on the *Pseudomonas*-free root surface, while high-mass organic species are enriched on the surface of *Pseudomonas* attachment spots.

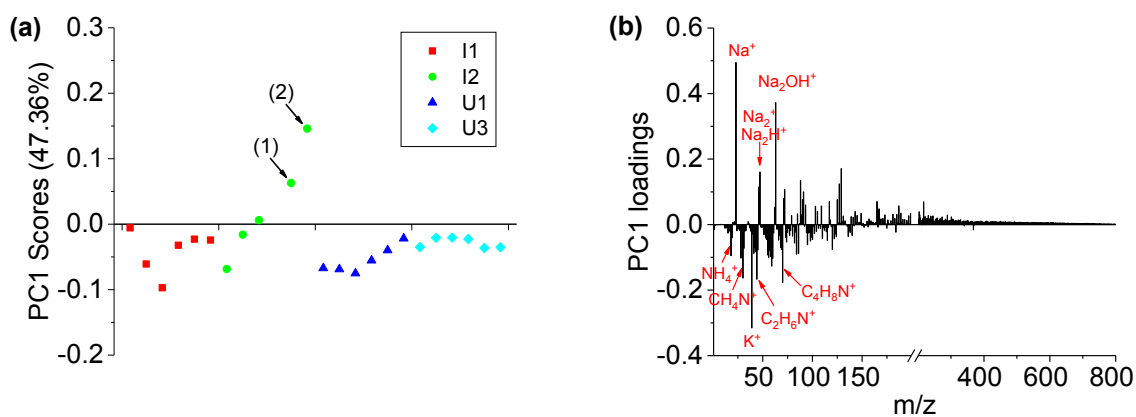


Figure 4. PCA analysis results of positive ion spectra of I1, I2, U1 and U3 samples. (a) PC1 scores plot; (b) PC1 loadings plot. It should be noted that the data spots (1) and (2) in (a) are corresponding to the two locations (1) and (2) in the Figure 1b, where *Pseudomonas* was observed.

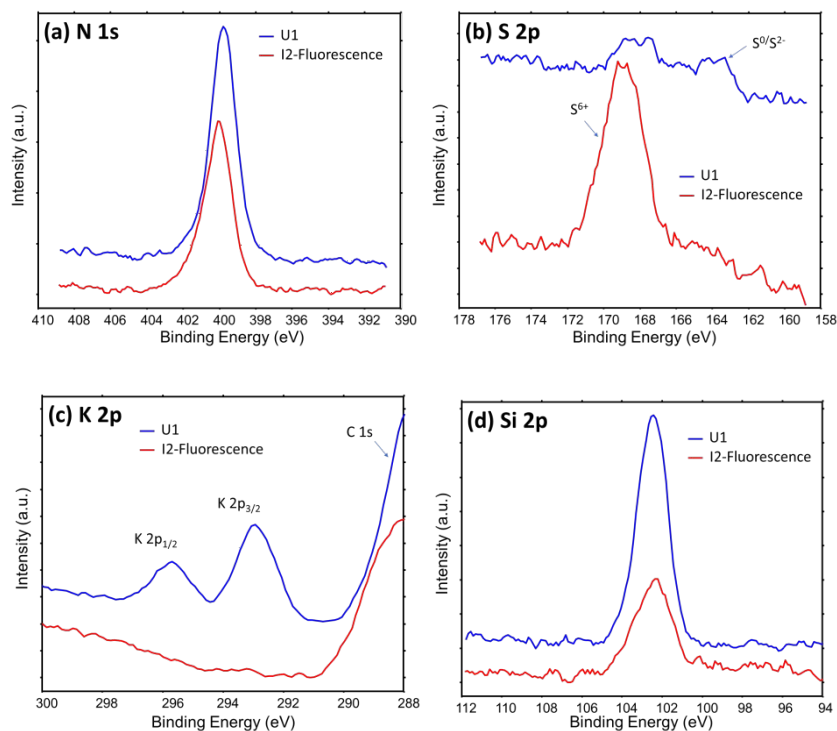
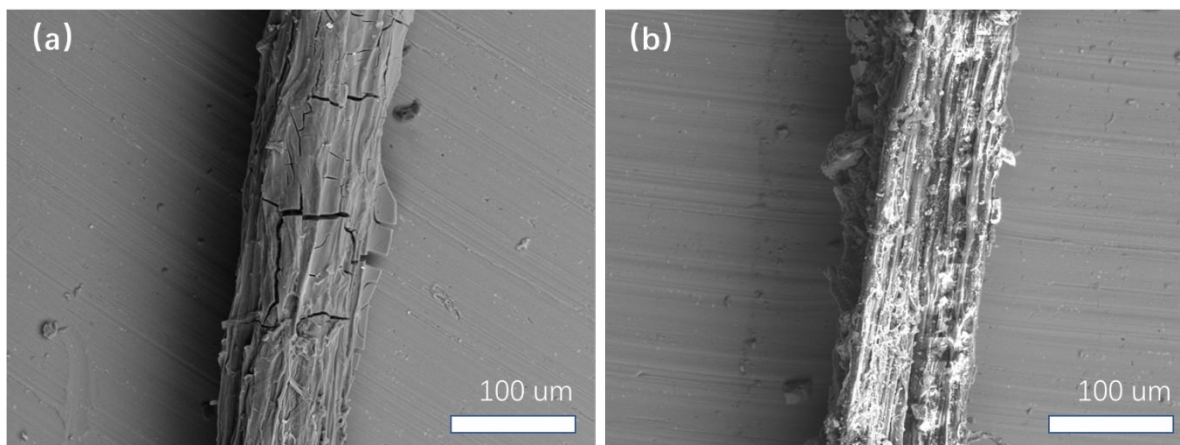


Figure 5. High energy resolution XPS data showing the chemical difference between *Pseudomonas*-free root surface (U1 plant) and the root surface of *Pseudomonas* attachment spots (I2 plant, location (1) in Figure 2b).

Figure 5 shows XPS data from two representative locations on the roots of the I2 and U1 plants. More N, K and Si were observed on *Pseudomonas*-free root surface, while more S was observed on *Pseudomonas* attachment spots. These results are well consistent with the results from ToF-SIMS/PCA analysis. For example, both XPS S spectra and PCA analysis results of ToF-SIMS negative ion spectra show more $-SO_x$ group on the surface of *Pseudomonas* attachment spots. Such a consistency is very reasonable, because both techniques are surface sensitive, sharing similar

1
2
3 information depth (a few nanometers) during analysis. It should be noted that XPS can provide
4 chemical state information, which cannot be obtained from fluorescence, SIMS and SEM analysis.
5 A notable observation in S 2p spectra (**Fig. 5b**) is two chemical states of S (S^{6+} and S^0/S^{2-}) on the
6 *Pseudomonas*-free root surface, but only one dominant chemical state of S (S^{6+}) on the
7 *Pseudomonas* attachment spots. One possible explanation for such an observation is that there was
8 some (~ 1 mM) of $MgSO_4$ in the growth medium for *Pseudomonas*, so that some SO_4^{2-} might stay
9 in the extracellular polymeric substances of the *Pseudomonas* biofilm.
10
11



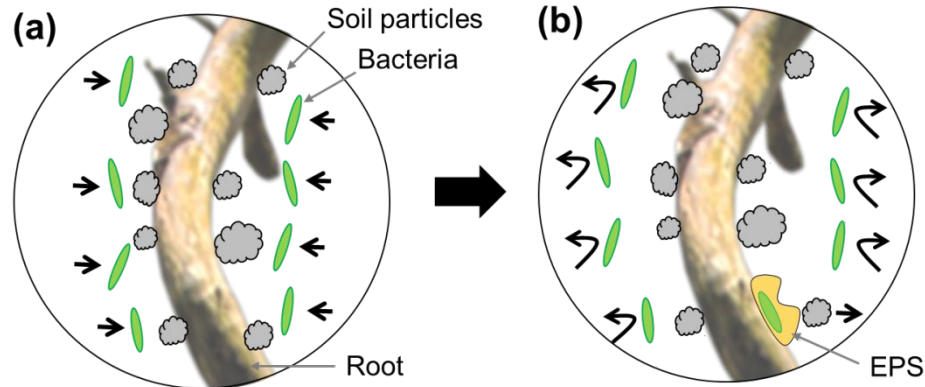
27
28 **Figure 6.** SEM images of root surfaces obtained after ToF-SIMS measurements. (a) Root surface from the I2 plant at
29 location (1) with *Pseudomonas* attachment shown in Fig. 1b; (b) *Pseudomonas*-free root surface on a root segment
30 from the U1 plant.

31
32 Figure 6 displays SEM images of roots with and without *Pseudomonas* attachment. The root
33 surface with *Pseudomonas* attachment looks smoother, almost free of soil particles. In contrast,
34 many small soil particles were observed on the *Pseudomonas*-free root surface. This situation is
35 agreement with the ToF-SIMS and XPS data that more Si and K (from soil mineral particles) on
36 the *Pseudomonas*-free root surface.
37

38
39 The above SEM observation is very interesting. From literature, biofilms are usually implicated in
40 aggregation processes because soil particles stick to them.³⁹ If so, a possible explanation for the
41 above observation is that *Pseudomonas* could only attach on soil particle-free areas. However,
42 SEM images show all root surfaces from U1 and U3 are with some considerable amount soil
43 particles, indicating that soil particle-free root surfaces are rare before *Pseudomonas* treatment. If
44 so, another possibility is that *Pseudomonas* attachment might reduce direct interactions between
45 root and soil particles.
46

47
48 It is notable that *Pseudomonas* attachment was observed only on two locations along the four root
49 segments from two *Pseudomonas*-inoculated *Brachypodium* plants (I1 and I2), i.e., locations (1)
50 and (2) of the I2 plant. One possible explanation for such an observation is that the *Pseudomonas*
51 treatment process was not uniform. However, this is doubtful since large amount of *Pseudomonas*
52 bacterial solution was added to the soil around the I1 and I2 plants, and root segments for imaging
53 were selected close to the inoculation site. A more plausible explanation is that direct interactions
54 between *Pseudomonas* cells and *Brachypodium* roots is weak and outcompeted by root-mineral
55 interactions (**Fig. 7a**). Such a weak interaction between *Pseudomonas* cells and *Brachypodium*
56
57

1
2
3 roots has been confirmed by a separate research in our lab.⁴⁰ In that work, the *Brachypodium* roots
4 grew in liquid media with glass beads (not in soil), in which *Pseudomonas* seemed to have
5 difficulty in attaching to free root surface in the media, but could aggregate on the glass bead-root
6 interface.⁴⁰ Therefore, we tend to believe that *Pseudomonas* may produce extracellular polymeric
7 substances to form a biofilm on a small amount of root surfaces and that the biofilm can physically
8 separate roots and soil particles (**Fig. 7b**).
9



25
26 **Figure 7.** Schematic representation of the behavior of *Pseudomonas* bacteria on the *Brachypodium* root surface. (a)
27 After *Pseudomonas* bacteria were added, cells attempt to contact the root surface. (b) The interactions between
28 *Pseudomonas* bacteria and the *Brachypodium* root are weak, and most bacteria fail to firmly attach to the root surface.
29 A small number of bacteria could stick to root surface forming extracellular polymeric substances (EPS) biofilm. The
30 biofilm would reduce the strong interactions between soil particles and the root surface.

31 Conclusions

32
33 Our data suggest that the root surface is a very inhomogeneous system, and chemical imaging tools
34 with sufficient spatial resolution (from nm to mm) are valuable in elucidating the complex
35 interactions at the plant-microbe, microbe-microbe, and plant-plant interfaces. Using a correlative
36 imaging approach comprised of fluorescence microscopy, ToF-SIMS, high-energy resolution XPS,
37 and SEM, and enabled by the development of a universal sample holder, we found that the
38 interaction between *Pseudomonas fluorescens* SBW25 and *Brachypodium distachyon* roots was
39 weak and confined to only few spots along the sampled root segments. Chemical imaging
40 supported by PCA analysis suggest that the bacterial attachment spots were enriched in Na- and
41 S-related and high-mass organic species, whereas the bacterial-free root surface was enriched in
42 N, K and Si species. We hypothesize that: 1) enrichment of N, K and Si on the *Pseudomonas*-free
43 root surface indicates the presence of soil particles; and 2) attachment of the *Pseudomonas* cells to
44 the root surface is outcompeted by strong root-soil mineral interactions but facilitated by formation
45 of EPS, as reflected by accumulation of high-mass organic species at the attachment spots. Given
46 the considerable interest in harnessing the plant microbiome for mitigating climate change and
47 improving plant productivity and health⁴¹⁻⁴⁵, it is critical that we obtain a comprehensive insight
48 into the mechanisms that govern plant-microbe interactions. We argue that the correlative surface
49 imaging strategy presented here offers great potential for our ability to understand, predict and
50 control rhizosphere interactions for desirable outputs.
51
52
53
54
55
56
57
58
59
60

Acknowledgements

This research was supported by the Department of Energy (DOE) Office of Biological and Environmental Research (BER) and was conducted at the Environmental Molecular Sciences Laboratory (EMSL), a DOE user facility, as a contribution to the EMSL Strategic Science Area under project 22142. The authors thank for helpful discussions with Professor Rene Boiteau in Oregon State University.

References:

1. Ahkami, A. H.; White III, R. A.; Handakumbura, P. P.; Jansson, C., Rhizosphere engineering: Enhancing sustainable plant ecosystem productivity. *Rhizosphere* **2017**, *3*, 233-243.
2. Bais, H. P.; Weir, T. L.; Perry, L. G.; Gilroy, S.; Vivanco, J. M., The role of root exudates in rhizosphere interactions with plants and other organisms. *Annu. Rev. Plant Biol.* **2006**, *57*, 233-266.
3. Ahemad, M.; Kibret, M., Mechanisms and applications of plant growth promoting rhizobacteria: Current perspective. *Journal of King Saud University - Science* **2014**, *26*, (1), 1-20.
4. Kloepper, J. W.; Leong, J.; Teintze, M.; Schroth, M. N., Enhanced plant growth by siderophores produced by plant growth-promoting rhizobacteria. *Nature* **1980**, *286*, (5776), 885-886.
5. Pieterse, C.; Van Wees, S.; Hoffland, E.; Van Pelt, J. A.; Van Loon, L. C., Systemic resistance in Arabidopsis induced by biocontrol bacteria is independent of salicylic acid accumulation and pathogenesis-related gene expression. *The Plant Cell* **1996**, *8*, (8), 1225-1237.
6. Yang, J.; Kloepper, J. W.; Ryu, C.-M., Rhizosphere bacteria help plants tolerate abiotic stress. *Trends in Plant Science* **2009**, *14*, (1), 1-4.
7. Zaidi, A.; Khan, M.; Ahemad, M.; Oves, M., Plant growth promotion by phosphate solubilizing bacteria. *Acta microbiologica et immunologica Hungarica* **2009**, *56*, (3), 263-284.
8. Otieno, N.; Lally, R. D.; Kiwanuka, S.; Lloyd, A.; Ryan, D.; Germaine, K. J.; Dowling, D. N., Plant growth promotion induced by phosphate solubilizing endophytic Pseudomonas isolates. *Frontiers in Microbiology* **2015**, *6*, 745.
9. Berg, G., Plant-microbe interactions promoting plant growth and health: perspectives for controlled use of microorganisms in agriculture. *Applied microbiology and biotechnology* **2009**, *84*, (1), 11-18.
10. Vejan, P.; Abdullah, R.; Khadiran, T.; Ismail, S.; Nasrulhaq Boyce, A., Role of Plant Growth Promoting Rhizobacteria in Agricultural Sustainability—A Review. *Molecules* **2016**, *21*, (5), 573.
11. Dey, R.; Pal, K. K.; Bhatt, D. M.; Chauhan, S. M., Growth promotion and yield enhancement of peanut (*Arachis hypogaea* L.) by application of plant growth-promoting rhizobacteria. *Microbiological Research* **2004**, *159*, (4), 371-394.
12. Compant, S.; Clément, C.; Sessitsch, A., Plant growth-promoting bacteria in the rhizo- and endosphere of plants: Their role, colonization, mechanisms involved and prospects for utilization. *Soil Biology and Biochemistry* **2010**, *42*, (5), 669-678.
13. Souza, R. d.; Ambrosini, A.; Passaglia, L. M., Plant growth-promoting bacteria as inoculants in agricultural soils. *Genetics and molecular biology* **2015**, *38*, (4), 401-419.
14. Brkljacic, J.; Grotewold, E.; Scholl, R.; Mockler, T.; Garvin, D. F.; Vain, P.; Brutnell, T.; Sibout, R.; Bevan, M.; Budak, H.; Caicedo, A. L.; Gao, C.; Gu, Y.; Hazen, S. P.; Holt, B. F.; Hong, S.-Y.; Jordan, M.; Manzaneda, A. J.; Mitchell-Olds, T.; Mochida, K.; Mur, L. A. J.; Park, C.-M.; Sedbrook, J.; Watt, M.; Zheng, S. J.; Vogel, J. P., Brachypodium as a Model for the Grasses: Today and the Future. *Plant Physiology* **2011**, *157*, (1), 3-13.
15. Scholthof, K.-B. G.; Irigoyen, S.; Catalan, P.; Mandadi, K. K., Brachypodium: A Monocot Grass Model Genus for Plant Biology. *The Plant Cell* **2018**, *30*, (8), 1673-1694.
16. Opanowicz, M.; Vain, P.; Draper, J.; Parker, D.; Doonan, J. H., Brachypodium distachyon: making hay with a wild grass. *Trends in Plant Science* **2008**, *13*, (4), 172-177.
17. Douché, T.; Clemente, H. S.; Burlat, V.; Roujol, D.; Valot, B.; Zivy, M.; Pont - Lezica, R.; Jamet, E., Brachypodium distachyon as a model plant toward improved biofuel crops: Search for secreted proteins involved in biogenesis and disassembly of cell wall polymers. *Proteomics* **2013**, *13*, (16), 2438-2454.
18. Do Amaral, F. P.; Pankiewicz, V. C.; Arisi, A. C. M.; de Souza, E. M.; Pedrosa, F.; Stacey, G., Differential growth responses of Brachypodium distachyon genotypes to inoculation with plant growth promoting rhizobacteria. *Plant molecular biology* **2016**, *90*, (6), 689-697.

19. Zhong, S.; Ali, S.; Leng, Y.; Wang, R.; Garvin, D. F., Brachypodium distachyon–Cochliobolus sativus pathosystem is a new model for studying plant–fungal interactions in cereal crops. *Phytopathology* **2015**, *105*, (4), 482-489.
20. Fitzgerald, T. L.; Powell, J. J.; Schneebeli, K.; Hsia, M. M.; Gardiner, D. M.; Bragg, J. N.; McIntyre, C. L.; Manners, J. M.; Ayliffe, M.; Watt, M., Brachypodium as an emerging model for cereal–pathogen interactions. *Annals of Botany* **2015**, *115*, (5), 717-731.
21. Figueroa, M.; Alderman, S.; Garvin, D. F.; Pfender, W. F., Infection of Brachypodium distachyon by formae speciales of Puccinia graminis: early infection events and host–pathogen incompatibility. *PLoS One* **2013**, *8*, (2), e56857.
22. Adesemoye, A.; Obini, M.; Ugoji, E., Comparison of plant growth-promotion with *Pseudomonas aeruginosa* and *Bacillus subtilis* in three vegetables. *Brazilian Journal of Microbiology* **2008**, *39*, (3), 423-426.
23. Rainey, P. B., Adaptation of *Pseudomonas fluorescens* to the plant rhizosphere. *Environmental Microbiology* **1999**, *1*, (3), 243-257.
24. Martínez-Viveros, O.; Jorquera, M.; Crowley, D.; Gajardo, G.; Mora, M., Mechanisms and practical considerations involved in plant growth promotion by rhizobacteria. *Journal of soil science and plant nutrition* **2010**, *10*, (3), 293-319.
25. Pham, V. T.; Rediers, H.; Ghequire, M. G.; Nguyen, H. H.; De Mot, R.; Vanderleyden, J.; Spaepen, S., The plant growth-promoting effect of the nitrogen-fixing endophyte *Pseudomonas stutzeri* A15. *Archives of microbiology* **2017**, *199*, (3), 513-517.
26. Zhu, B.; Gutknecht, J. L. M.; Herman, D. J.; Keck, D. C.; Firestone, M. K.; Cheng, W., Rhizosphere priming effects on soil carbon and nitrogen mineralization. *Soil Biology and Biochemistry* **2014**, *76*, 183-192.
27. Kaplan, D. I.; Xu, C.; Huang, S.; Lin, Y.; Tolić, N.; Roscioli-Johnson, K. M.; Santschi, P. H.; Jaffé, P. R., Unique organic matter and microbial properties in the rhizosphere of a wetland soil. *Environmental science & technology* **2016**, *50*, (8), 4169-4177.
28. Shi, S.; Nuccio, E. E.; Shi, Z. J.; He, Z.; Zhou, J.; Firestone, M. K., The interconnected rhizosphere: high network complexity dominates rhizosphere assemblages. *Ecology letters* **2016**, *19*, (8), 926-936.
29. Barahona, E.; Navazo, A.; Yousef - Coronado, F.; Aguirre de Cárcer, D.; Martínez - Granero, F.; Espinosa - Urgel, M.; Martín, M.; Rivilla, R., Efficient rhizosphere colonization by *Pseudomonas fluorescens* f113 mutants unable to form biofilms on abiotic surfaces. *Environmental microbiology* **2010**, *12*, (12), 3185-3195.
30. Guerrero-Molina, M. F.; Winik, B. C.; Pedraza, R. O., More than rhizosphere colonization of strawberry plants by *Azospirillum brasilense*. *Applied Soil Ecology* **2012**, *61*, 205-212.
31. Keiluweit, M.; Bougoure, J. J.; Nico, P. S.; Pett-Ridge, J.; Weber, P. K.; Kleber, M., Mineral protection of soil carbon counteracted by root exudates. *Nature Climate Change* **2015**, *5*, (6), 588-595.
32. Benninghoven, A., Chemical-Analysis of Inorganic and Organic-Surfaces and Thin-Films by Static Time-of-Flight Secondary-Ion Mass-Spectrometry (ToF-Sims). *Angew Chem Int Edit* **1994**, *33*, (10), 1023-1043.
33. Branson, O.; Bonnin, E. A.; Perea, D. E.; Spero, H. J.; Zhu, Z. H.; Winters, M.; Honisch, B.; Russell, A. D.; Fehrenbacher, J. S.; Gagnon, A. C., Nanometer-Scale Chemistry of a Calcite Biomineralization Template: Implications for Skeletal Composition and Nucleation. *P Natl Acad Sci USA* **2016**, *113*, (46), 12934-12939.
34. Graham, D. J.; Castner, D. G., Multivariate Analysis of ToF-SIMS Data from Multicomponent Systems: The Why, When, and How. *Biointerphases* **2012**, *7*, (1-4), 49.
35. Graham, D. J.; Wagner, M. S.; Castner, D. G., Information from complexity: Challenges of TOF-SIMS data interpretation. *Appl Surf Sci* **2006**, *252*, (19), 6860-6868.

- 1
2
3 36. Ding, Y. Z.; Zhou, Y. F.; Yao, J.; Xiong, Y. J.; Zhu, Z. H.; Yu, X. Y., Molecular evidence of a toxic
4 effect on a biofilm and its matrix. *Analyst* **2019**, *144*, (8), 2498-2503.
- 5 37. Ding, Y. Z.; Zhou, Y. F.; Yao, J.; Szymanski, C.; Fredrickson, J.; Shi, L.; Cao, B.; Zhu, Z. H.; Yu, X. Y.,
6 In Situ Molecular Imaging of the Biofilm and Its Matrix. *Anal Chem* **2016**, *88*, (22), 11244-11252.
- 7 38. Hua, X.; Yu, X. Y.; Wang, Z. Y.; Yang, L.; Liu, B. W.; Zhu, Z. H.; Tucker, A. E.; Chrisler, W. B.; Hill, E.
8 A.; Thevuthasan, T.; Lin, Y. H.; Liu, S. Q.; Marshall, M. J., In situ molecular imaging of a hydrated biofilm
9 in a microfluidic reactor by ToF-SIMS. *Analyst* **2014**, *139*, (7), 1609-1613.
- 10 39. Costa, O. Y. A.; Raaijmakers, J. M.; Kuramae, E. E., Microbial Extracellular Polymeric Substances:
11 Ecological Function and Impact on Soil Aggregation. *Front Microbiol* **2018**, *9*, 1636
- 12 40. Boiteau, R. M.; Markillie, L. M.; Mitchell, H.; Hu, D.; Chu, R.; Hoyt, D.; Pasa-Tolic, L.; Jansson, J.;
13 Jansson, C., Phytosiderophore piracy by soil bacteria. Submitted to ISME Journal.
- 14 41. Busby, P. E.; Soman, C.; Wagner, M. R.; Friesen, M. L.; Kremer, J.; Bennett, A.; Morsy, M.; Eisen,
15 J. A.; Leach, J. E.; Dangl, J. L., Research priorities for harnessing plant microbiomes in sustainable
16 agriculture. *Plos Biol* **2017**, *15*, (3).
- 17 42. Sergaki, C.; Lagunas, B.; Lidbury, I.; Gifford, M. L.; Schafer, P., Challenges and Approaches in
18 Microbiome Research: From Fundamental to Applied. *Front Plant Sci* **2018**, *9*, 1205.
- 19 43. Vorholt, J. A.; Vogel, C.; Carlstrom, C. I.; Muller, D. B., Establishing Causality: Opportunities of
20 Synthetic Communities for Plant Microbiome Research. *Cell Host Microbe* **2017**, *22*, (2), 142-155.
- 21 44. Lau, J. A.; Lennon, J. T.; Heath, K. D., Trees harness the power of microbes to survive climate
22 change. *P Natl Acad Sci USA* **2017**, *114*, (42), 11009-11011.
- 23 45. Yu, P.; Hochholdinger, F., The Role of Host Genetic Signatures on Root-Microbe Interactions in
24 the Rhizosphere and Endosphere. *Front Plant Sci* **2018**, *9*, 1896.
- 25
26
27
28
29
30
31
32
33
34
35
36
37
38
39
40
41
42
43
44
45
46
47
48
49
50
51
52
53
54
55
56
57
58
59
60